AD-A173 961 CONVERGENCE ANALYSIS AND ACCELERATION OF THE SCHWARTZ ALTERNATING METHOD (U) STANFORD UNIV CA CENTER FOR LARGE SCALE SCIENTIFIC COMPUTATIO J OLIGER ET AL. 1/1

UNCLASSIFIED 26 AUG 86 CLASSIC-86-12 N00014-75-C-1132 F/G 12/1 NL

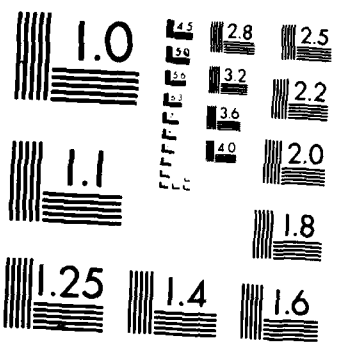

'CROCOPY RESOLUTION TEST CHART
NATIONAL BUREAU OF STANDARDS 1963-A

15

CLaSSiC Project
Manuscript CLaSSiC-86-12

August 1986

Convergence Analysis and Acceleration of the Schwarz Alternating Method

Joseph Oliger
William Skamarock
Wei–Pai Tang

AD-A173 961

DTIC
ELECTE
NOV 1 4 1986
S D
E

OTIC FILE COPY

Center for Large Scale Scientific Computation
Building 460, Room 313
Stanford University
Stanford, California 94305

This document has been approved for public release and sale; its distribution is unlimited.

86 11 4 017

Convergence Analysis and Acceleration of the Schwarz Alternating Method

Joseph Oliger
William Skamarock
Wei-Pai Tang[1]

20 December 1985
Revised 26 August 1986

Accession For
NTIS GRA&I
DTIC TAB
Unannounced
Justification per ltr
By
Distribution/
Availability Codes
Dist | Avail and/or Special
A-1

[1]The authors have been supported during this project by the office of Naval Research under contracts N00014-75-C-1132 and N00014-84-K-0267

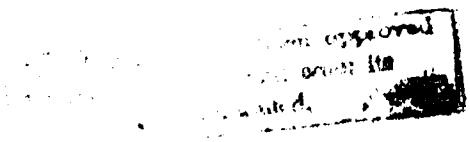

Abstract

The convergence rate of the Schwarz Alternating Method ($\bar{S}_A\bar{M}$) is studied for applications involving the solution of elliptic equations on composite grids. Such problems arise when solvers which can only be used on special domains, such as rectangles, are used for more general region; and in the disection of problems for parallel processing. It is shown that the convergence rate is a function of the overlap, number and shape of the subregions into which the problem domain is divided. The convergence rates for S_AM are slow and an accelerated method based on overrelaxation techniques is developed. The S_AM analysis is extended to predict the performance of the accelerated method and optimal relaxation parameters. Finally, we study the effects of changing the iteration order for the S_AM and accelerated S_AM methods

1 Introduction

The Schwarz Alternating Method (SAM) was initially introduced to obtain theoretical results for elliptic partial differential equations [Sch69]. This same idea has subsequently been used to develop algorithms for the numerical solution of the same class of problems (see [Tan86]). This work has been largely limited to problems in two dimensions and to breaking up the problem domain into limited numbers of components. The main motivation for using the method has been to deal with geometrical difficulties—to reduce the problem of solving on a complicated domain to a sequence of problems on simple domains. This has often been motivated by a desire to use special solvers that can only be used on regions of special shape, such as rectangles. These results confirm the applicability of the method, but show that the original iteration is limited in its effectiveness, its convergence rate is slow.

Our interest in the method has come from a need to solve elliptic equations on composite grids generated to both resolve complicated geometries and to adaptively resolve the solution [CFO85]. A technique is needed in this situation which allows one to use a standard software interface for each of the regions, such as solving on a sequence of rectangles, and which minimizes the communication required between the solution processes on the subregions. In this application we may have large numbers of subgrids in our composite grids. We are also interested in using the same technique to break up the global solution process into loosely coupled subtasks for parallel processing. This can also lead to large numbers of subgrids.

We have begun with a study of the convergence rate of the original Schwarz iteration as a function of the amount of overlap of the subgrids. This extends the earlier work of Miller [Mil65] to domains in R^p and to arbitrary numbers of subgrids. This is discussed in Section 2. The analysis is carried out by first showing that Schwarz iteration can be formulated as a block Gauss–Seidel iteration of a modified system of equations. The convergence rate is found to be exponential in both the amount of overlap and in the number of regions.

Since the convergence rates of the original iteration are slow and lead to inefficient algorithms, we consider a modification of the algorithms where we use an overrelaxation technique for the boundary values. This iteration is

described in section 3, and the results of a number of numerical experiments are presented. It is found that the strong dependence of the convergence rate on both the amount of overlap and on number of subregions can be greatly reduced resulting in acceptable performance. It is demonstrated that the optimal overrelaxation parameter can be successfully estimated using a formula due to Young [You71]. The sensitivity of the optimal overrelaxation parameter as a function of overlap and the number of grid parameters is also studied. Finally, we also study the effect of changing the order in which the iterations are carried out and introduce a red-black iteration which can be used for parallel processing whereas the sequential or Gauss–Seidel iteration cannot. Fortunately, it is found that the red-black iteration can be used successfully. Tables of data which illustrate optimal choices of overlap which minimize operations are also included.

2 Convergence as a Function of Overlap

The numerical Schwarz algorithm is essentially the same as the block Gauss–Seidel method for a modified matrix equation which has the same solution as the original finite element or finite difference equations of the elliptic partial differential equation. The relationship between the convergence of Schwarz Alternating Method (or $\mathcal{SAM}$) and the area of overlap has been observed previously. Miller [Mil65] proved a result for the case of two overlapping rectangles, see also G. Starius [Sta77] and E. Volkov [Vol68]. Miller was mainly interested in solving elliptic equations in irregular regions, an analysis for situations which arise in applications motivated by parallel processing and composite grids has not been carried out. Here we will show how overlapping affects the convergence of the $\mathcal{SAM}$ for model problems in the p–dimensional case. Before we consider the more general cases, it is easier to illustrate the analysis for a one–dimensional problem. The model problem we consider in one dimension is

$$y''(x) = f(x), \qquad x \in (0,1)$$

$$y(0) = \alpha; \quad y(1) = \beta.$$

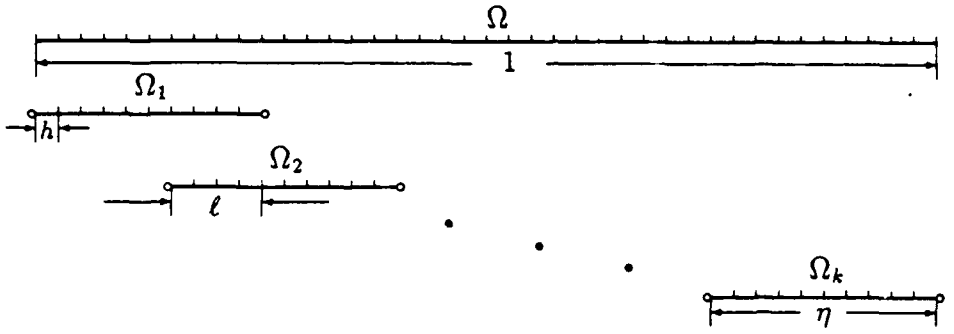

Figure 1: One dimensional overlapping grid.

After discretization using a centered second order method the resulting linear system is

$$T_n x = b, \tag{1}$$

where

$$T_n = Tridiagonal\{1, \quad -2, \quad 1\}_{n \times n}.$$

The SAM for solving this problem divides the region into k overlapping subregions Ω_i $i = 1, \cdots, k$ as shown in Figure 1. (To simplify the analysis we assume the overlapping pattern is uniform, similar conclusions can be deduced for more general problems.)

Let h be the grid size, ℓ the length of the overlap and η the length of every subregion. Then $n = \frac{1}{h}$, $l = \frac{\ell}{h}$ and $m = \frac{\eta}{h}$. The circular points in Figure 1 are new boundaries for the subregions. A natural way to implement SAM is to first guess some "reasonable" initial values for the artificial boundaries and then to solve these subproblems separately. Next, use the solutions of these subproblems to update the values on the artificial boundaries and proceed iteratively until the solutions on the overlapping regions converge. If we solve on these subregions in a natural order, each succeeding subregion takes its new boundary values from the new solution of the previous subregion. This procedure is equivalent to applying the block Gauss-Seidel

method to the following modified matrix problem:

$$\tilde{T}\tilde{x} = \begin{bmatrix} T_m & F_m & & & & & \\ E_m & T_m & F_m & & & & \\ & \ddots & \ddots & \ddots & & & \\ & & \ddots & \ddots & \ddots & & \\ & & & \ddots & \ddots & \ddots & \\ & & & & E_m & T_m & F_m \\ & & & & & E_m & T_m \end{bmatrix} \tilde{x} \qquad (2)$$

$$= (T_m \otimes I_k + E_m \otimes L_k + F_m \otimes U_k)\tilde{x} = \tilde{b}.$$

The corresponding block Gauss-Seidel iteration for this equation is as follows:

$$(E_m \otimes L_k + T_m \otimes I_k)\tilde{x}^{(k+1)} = -(F_m \otimes U_k)\tilde{x}^{(k)} + \tilde{b}.$$

The quantities above are defined as:

- E_m: an $m \times m$ matrix with zero elements everywhere except for 1 in position $(1, m-l+1)$.
- F_m: an $m \times m$ matrix with zero elements everywhere except 1 in position (m, l).
- I_k: a $k \times k$ identity matrix.
- L_k: a $k \times k$ matrix with zero elements everywhere except for 1's on the subdiagonal.
- U_k: a $k \times k$ matrix with zero elements everywhere except for 1's on the superdiagonal.

It can be shown that (1) and (2) are equivalent (see [Tan86]). Therefore, the convergence analysis of the SAM is reduced to calculating the eigenvalues of the block Jacobi matrix $J = M^{-1}N$ where

$$\begin{aligned} M &= T_m \otimes I_k, \\ N &= E_m \otimes L_k + F_m \otimes U_k. \end{aligned}$$

If we multiply out $M^{-1}N$ then

$$\begin{aligned} J &= (T_m \otimes I_k)^{-1}(E_m \otimes L_k + F_m \otimes U_k) \\ &= (T_m^{-1} \otimes I_k)(E_m \otimes L_k + F_m \otimes U_k) \\ &= (T_m^{-1}E_m) \otimes L_k + (T_m^{-1}F_m) \otimes U_k \\ &= \tilde{E}_m \otimes L_k + \tilde{F}_m \otimes U_k, \end{aligned}$$

where $\tilde{E}_m$ and $\tilde{F}_m$ have almost all zero elements except columns $(m-l+1)$ and l, respectively. It is clear that the rank of this matrix is at most $2k$. After some row and column exchanges J can be transformed to $\tilde{J}$, which is similar to J:

$$\tilde{J} = UJU^T = \begin{bmatrix} 0_{(n-2k)\times(n-2k)} & C_{(n-2k)\times 2k} \\ 0_{2k\times(n-2k)} & G_{2k\times 2k} \end{bmatrix},$$

where

$$G = D' \otimes I_k + E' \otimes L_k + F' \otimes U_k,$$

$$E' = \begin{bmatrix} a & 0 \\ 0 & 0 \end{bmatrix}, \quad D' = \begin{bmatrix} 0 & b \\ b & 0 \end{bmatrix}, \quad F' = \begin{bmatrix} 0 & 0 \\ 0 & a \end{bmatrix},$$

$$a = \frac{l}{(m+1)}, \quad b = \frac{m+1-l}{(m+1)}.$$

It is clear that $\lambda_J \in (0 \cup \lambda_G)$, where λ_J and λ_G are the eigenvalues of matrices J and G, respectively.

Theorem 2.1 *If $a \leq 0.5$ then λ_G satisfies the following equations:*

$$\lambda_G^2 + 2 * a * \cos\theta * \lambda_G - a^2 + b^2 = 0,$$

$$\lambda_G * \sin(k * \theta) = a * \sin((k-1) * \theta)$$

where θ is a parameter [Tan86].

Let

$$\rho = max\{|\ \lambda_G\ |\} = max\{|\ \lambda_J\ |\},$$

it is easy to show: if $k = 2$

$$\rho = b,$$

if $k = 3$

$$\rho = \sqrt{b}.$$

Now we can immediately observe some important facts about S_4^M :

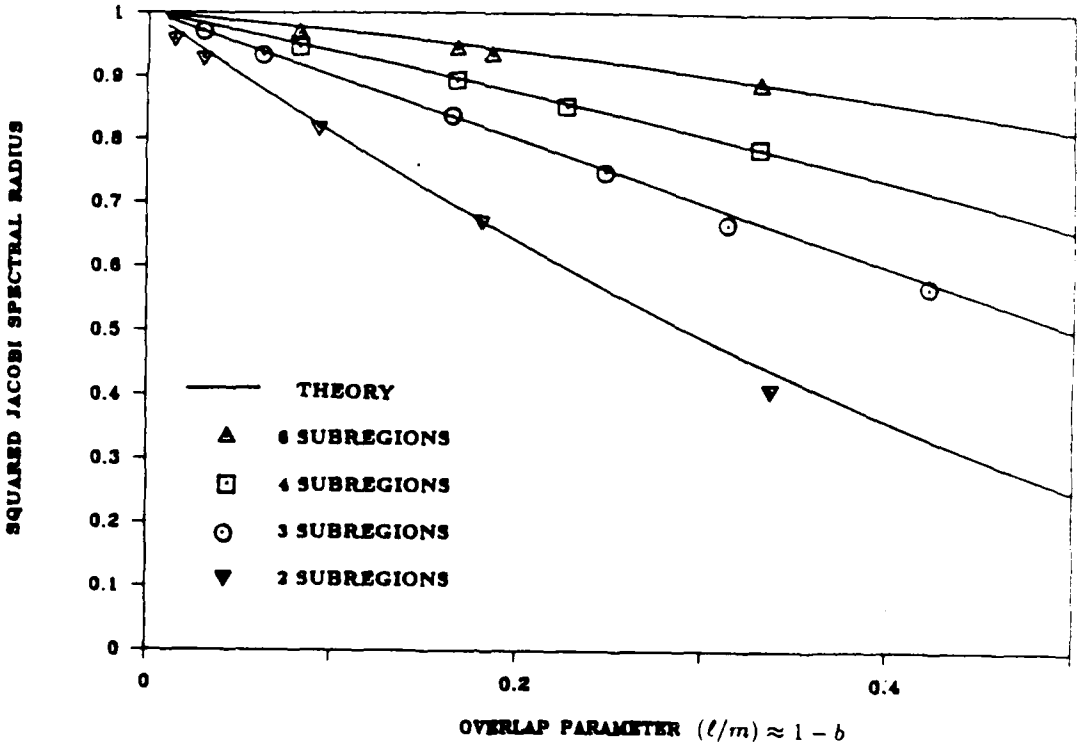

Figure 2: Theoretical and computational values of the squared spectral radius for the block Jocobi iteration matrix in the 1–D case. Increasing $\kappa = l/m$ corresponds to increasing overlap.

1. First, the spectral radius of J only depends on the number of subregions k and the overlapping area a. This means that the convergence of S_H^M is independent of mesh size h.

2. For the case of $k = 2$ and 3, we notice that when the overlapping area increases, ρ decreases, and when k increases ρ increases. These conclusions also are valid for the general case ($k > 3$). We cannot give a closed form solution for k greater than 5 but the numerical results indicate that similar results hold(see Figure 2).

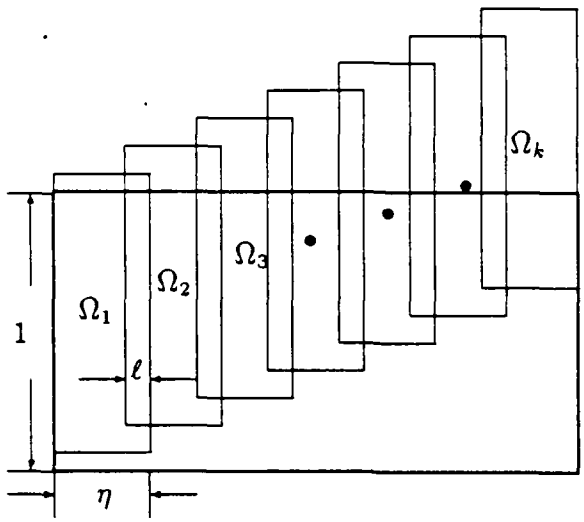

Figure 3: Two dimensional overlapping grid. The subregions are shifted upwards to improve visibility of the overlapping pattern

A similar analysis can be applied to the model problem in 2 dimensions. The Poisson equation in two–dimensions is:

$$\frac{\partial^2 U}{\partial x^2} + \frac{\partial^2 U}{\partial y^2} = f(x,y), \qquad (x,y) \in (0,1) \times (0,1). \tag{3}$$

Using central differences we obtain a discretization of this equation:

$$Ax = b, \tag{4}$$

where

$$A = T_n \otimes I_n + I_n \otimes T_n.$$

This is of the same form as we obtained in the one–dimensional case, h is the mesh size and $n = \frac{1}{h}$. If we cover (0,1) on the x axis with k subregions as in the one–dimensional case, then the solution area is covered by k overlapping rectangles as shown above.

If we apply S_4^M to these overlapping subregions, then it is equivalent to applying the Gauss-Seidel method to the following modified equation:

$$\tilde{A}\tilde{x} = \begin{bmatrix} W_m & F'_m & & & & & \\ E'_m & W_m & F'_m & & & & \\ & \ddots & \ddots & \ddots & & & \\ & & \ddots & \ddots & \ddots & & \\ & & & \ddots & \ddots & \ddots & \\ & & & & E'_m & W_m & F'_m \\ & & & & & E'_m & W_m \end{bmatrix}_{k\times k} \tilde{x} \qquad (5)$$

$$= \{W_m \otimes I_k + I_n \otimes E_m) \otimes L_k + (I_n \otimes F_m) \otimes U_k\}\tilde{x} = \tilde{b},$$

where

$$W_m = T_n + I_m + I_n + T_m, \quad E'_m = I_n \otimes E_m, \quad F'_m = I_n \otimes F_m.$$

In order to analyze the convergence of S_4^M, we need to study the spectral radius of the block Jacobi iterative matrix derived from the matrix $\tilde{A}$:

$$J = M^{-1}N,$$

where

$$M = W_m \otimes I_k, \qquad N = (I_n \otimes E_m) \otimes L_k + (I_n \otimes F_m) \otimes U_k.$$

Then we have the following result:

Theorem 2.2 *The matrix J is similar to the matrix*

$$D = \begin{bmatrix} 0_{n^2-2nk\times n^2-2nk} & C_{n^2-2nk\times 2nk} \\ 0_{2nk\times n^2-2nk} & G_{2nk\times 2nk} \end{bmatrix},$$

where

$$G = Block - diagonal\{G_i\}, \quad i = 1, \cdots, n,$$

$$G_i = D'_i \otimes I_k + E'_i \otimes L_k + F'_i \otimes U_k,$$

$$E'_i = \begin{bmatrix} \alpha_i & 0 \\ 0 & 0 \end{bmatrix}, \quad D'_i = \begin{bmatrix} 0 & \beta_i \\ \beta_i & 0 \end{bmatrix}, \quad F'_i = \begin{bmatrix} 0 & 0 \\ 0 & \alpha_i \end{bmatrix},$$

$$\alpha_i = \frac{\zeta_i^{\kappa m} - \zeta_i^{-\kappa m}}{\zeta_i^m - \zeta_i^{-m}}, \quad \beta_i = \frac{\zeta_i^{(1-\kappa)m} - \zeta_i^{-(1-\kappa)m}}{\zeta_i^m - \zeta_i^{-m}}, \quad i = 1, \cdots, n \ ,$$

$$\zeta_i = \nu_i + \sqrt{\nu_i^2 - 1}, \quad \nu_i = 2 - \cos(\frac{i\pi}{n+1}), \quad i = 1, \cdots, n \ ,$$

and $\kappa = l/m$ *is the ratio of the overlap.*

Proof. Let

$$U = (X_n \otimes I_m) \otimes I_k$$

where X_n is an orthogonal matrix for which the columns are the eigenvectors of the matrix T_n, and U is an orthogonal matrix. Note $UNU^T = N$. Then

$$\begin{aligned} J' = UJU^T &= UM^{-1}NU^T \\ &= (UMU^T)^{-1}N \\ &= \{((X_nT_nX_n^T \otimes I_m) + I_n \otimes T_m)^{-1} \otimes I_k\}N \\ &= \{(D_n \otimes I_m + I_n \otimes T_m)^{-1} \otimes I_k\}N \ , \end{aligned}$$

where D_n is a diagonal matrix whose diagonal elements are the eigenvalues of T_n. We know that there is an $mn \times mn$ permutation matrix P such that

$$P(A \otimes B)P^T = B \otimes A$$

where A and B are any $n \times n$ and $m \times m$ matrices, respectively. So we have

$$P(I_n \otimes E_m)P^T = E_m \otimes I_n, \quad P(I_n \otimes F_m)P^T = F_m \otimes I_n,$$

$$P(D_n \otimes I_m + I_n \otimes T_m)P^T = I_m \otimes D_n + T_m \otimes I_n.$$

Notice that:

$$\begin{aligned} Q &= I_m \otimes D_n + T_m \otimes I_n \\ &= Block\text{-}diagonal\{\tilde{T}_i\}_{n\times n}, \\ \tilde{T}_i &= Tridiagonal\{1, \gamma_i, 1\}_{m\times m}, \\ \gamma_i &= 4 + 2\cos(\frac{i\pi}{n+1}), \quad i = 1, \cdots, n. \end{aligned}$$

Let $\tilde{P} = P \otimes I_k$, Then we have

$$\begin{aligned} J'' &= \tilde{P}J'\tilde{P}^T = \tilde{P}\{(D_n \otimes I_m + I_n \otimes T_m)^{-1} \otimes I_k\}\tilde{P}^T\tilde{P}N\tilde{P}^T \\ &= \{(P(D_n \otimes I_m + I_n \otimes T_m)P^T)^{-1} \otimes I_k\}\{(E_m \otimes I_n) \otimes L_k + (F_m \otimes I_n) \otimes U_k\} \\ &= (Q^{-1} \otimes I_k)\{(E_m \otimes I_n) \otimes L_k + (F_m \otimes I_n) \otimes U_k\} \\ &= (\tilde{E}_m \otimes I_n) \otimes L_k + (\tilde{F}_m \otimes I_n) \otimes U_k \end{aligned}$$

As in the one–dimensional analysis, we can move all of the non-zero columns to the last columns and the theorem follows.

Since the structures of these diagonal blocks are the same as those analyzed in the one–dimensional case, we can find a similarly tight estimate of the spectral radius of J, ρ_J, by using Theorem 1. But here it is clear that

$$\alpha_i + \beta_i < 1, \quad \alpha_i > 0, \quad \beta_i > 0 \quad i = 1, \cdots, n$$

and thus we cannot derive a closed form for ρ_J, but we may use the Gershgorin theorem to get a bound for ρ_J.

Corollary 1

$$\rho_J \leq \alpha_1 + \beta_1.$$

If we denote $\mu = \frac{m}{n}$, it is easy to estimate the asymptotic bound for ρ_J(as $h \to 0$):

Corollary 2 *If* $k = 2$,

$$\rho_J \leq \frac{\sinh((1-\kappa)\mu\pi)}{\sinh(\mu\pi)}.$$

If $k > 2$

$$\rho_J \leq \frac{\sinh(\kappa\mu\pi) + \sinh((1-\kappa)\mu\pi)}{\sinh(\mu\pi)}.$$

The relationship between ρ_J and the two parameters l and μ is shown in Figure 4.

Similar results can be derived for model problems in more dimensions.

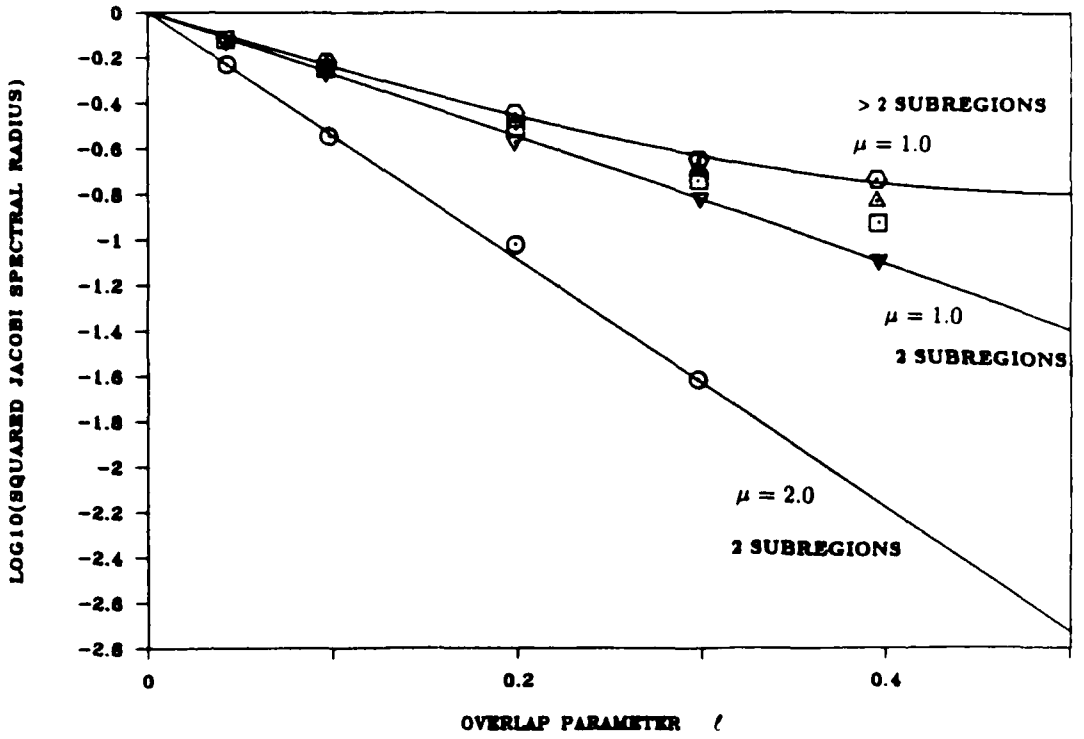

Figure 4: Theoretical bounds and computational values of the squared spectral radius for the block Jocobi iteration matrix in the 2-D case. Increasing ℓ corresponds to increasing overlap. Note that the domain size increases with increasing overlap when the subregion size is held fixed.

Theorem 2.3 *For the p-dimensional model problem the asymptotic bound for the spectral radius of the block Jacobi iterative matrix is:*

$$\rho_J \leq \frac{\sinh(\sqrt{p-1}\kappa\mu\pi) + \sinh(\sqrt{p-1}(1-\kappa)\mu\pi)}{\sinh(\sqrt{p-1}\mu\pi)}$$

Here we use the same notation as used for the one–dimensional case: $l = \frac{\ell}{h}$, $m = \frac{\eta}{h}$, $\kappa = \frac{l}{m}$ and $\mu = \frac{m}{n}$.

The same analysis can be applied to the nine–point stencil or tensor product finite-element schemes which have higher accuracy. The latter need some more complicated eigenvalue analysis. We will not list all of these results here, but our results indicate that the relationship between the convergence of S_A^M and the overlapped area, and the relationship between convergence and the number of the subregions is similar. All these results guide us to more efficient implementations of the S_A^M.

3 Numerical Results and Over Relaxation

Numerical experiments were performed to verify the theoretical results of the previous section and also to search for methods which more efficiently solve the overlapping grid problem. The 1-D model problem (1) and the 2-D Poisson equation (4) are solved numerically using the S_A^M . Convergence of the numerical solution to the exact solution is measured by calculating the l_1, l_2 and l_∞ norms of the solution error. These norms are defined by

$$\begin{aligned}
\|U\|_1 &= \sum_{i,j} \mid \tilde{u}_{i,j} - u_{i,j} \mid \Delta x \Delta y \\
\|U\|_2 &= \left[\sum_{i,j} \mid \tilde{u}_{i,j} - u_{i,j} \mid^2 \Delta x \Delta y \right]^{1/2} \\
\|U\|_\infty &= \max_{i,j} \mid \tilde{u}_{i,j} - u_{i,j} \mid
\end{aligned}$$

where $\tilde{u}_{i,j}$ is the exact solution.

We solved the one and two dimensional problems calculating the error norms at each iteration of the S_A^M . The solution error norms all decay exponentially at the same rate, this decay being of the form

$$\|\epsilon^{(k)}\|_i = \|\epsilon^{(0)}\|_i \varrho^k$$

where k is the iteration number. The constant ϱ is the convergence factor and estimates of it should compare with the theoretical results for the spectral radius of the G-S iterative matrix (2). The theoretical estimates of the previous section were for the iterative Jacobi matrix but the G-S spectral radius is the square of the Jacobi spectral radius (Varga, 1962). Hence, we can directly compare the theoretical and experimental results.

Figure 3 is a plot of the theoretical estimates of the spectral radii of the G-S iterative matrix and the experimental convergence factor versus the nondimensional overlap l/m for the 1-D problem with 2, 3, 4 and 6 subregions. Theory and computation compare well, especially at the smaller overlaps (larger values of b). As the theory indicates, the Jacobi spectral radii provide an upper bound on the convergence factors and the convergence factors increase with smaller overlaps.

Two dimensional $\mathcal{SAM}$ problems are characterized by two parameters, μ and l. Corollary 2 gives expressions for the spectral radii of the two subregion iterative matrix, and also an upper bound on the spectral radii for more than two subregions. The theoretical prediction of the spectral radii for the G-S iterative matrix along with numerically determined decay rates for the 2-D $\mathcal{SAM}$ problem are shown in Figure 4. The relative grid ratio μ is held constant and the relative overlap l is varied for the 2, 3, 4 and 6 subregion $\mathcal{SAM}$ problem. Once again computations and theory agree. The behavior in the 2-D case is similar to that of the 1-D case with the convergence factors increasing for smaller overlaps. The theory also correctly predicts the behavior of the convergence factor for different grid shapes as can be seen in the agreement between theory and observations for the μ equal to two case.

The monotonic, exponential decay of the error norms indicates that some form of overrelaxation may be suitable for increasing the convergence rate of the numerical solution to the true solution. One possible scheme is to overrelax at the boundaries of the subregions. If u is a boundary value of region two and lies in region one then we could set this boundary value using

$$u^{(k)} = u^{(k-1)} + \omega(\tilde{u}^{(k)} - u^{(k-1)}) \tag{6}$$

where k is the $\mathcal{SAM}$ iteration step and $\tilde{u}$ is the value obtained from the latest solution on region one. The overrelaxation parameter is ω . $\omega = 1$ produces

no relaxation and typically $1 < \omega < 2$ This can be thought of as using $\mathcal{SAM}$ with SOR (Successive Over Relaxation).

The results obtained using the overrelaxed $\mathcal{SAM}$ are impressive. Figures 5 and 6 show the relative work used to obtain an error of less than 10^{-5} (as measured by the convergence norms) using no relaxation factor and also using a optimal relaxation factor for the 1-D – two, three, four and six subregion cases. As the overlap becomes smaller the gain using the overrelaxed $\mathcal{SAM}$ becomes greater. However, the total amount of work necessary to obtain a converged solution is now only weakly dependent on overlap. Table 1 lists the overrelaxation parameters used in these cases. Figures 7 and 8 along with Table 2 contain results for the 2-D model problem. For the 2-D problem, all the points along an inner boundary are overrelaxed using (6). The 2-D results do not show as dramatic savings in computational effort as are found in the 1-D case; but the savings are still very significant, usually cutting the amount of work in half.

As in other applications of relaxation techniques, the critical task is choosing the relaxation parameter omega. Figure 9 is a plot of the relative work versus the value of omega for various 1 and 2-D, n subregion $\mathcal{SAM}$ problems. **As the amount of overlap decreases the computational savings, optimal omega and the sensitivity of the savings to the choice of omega all increase.** The sensitivity of the computational savings to the choice of omega is much smaller in the 2-D problem compared to the 1-D problem. As we would expect, the choice of omega is most critical when the possible savings are greatest.

Since matrix $\tilde{A}$ in equation (5) has the property $A^{(\pi)}$[You71], we can use the following formula for the calculation of an optimal overrelaxation factor given the spectral radius of the Jacobi iterative matrix.

$$\omega_{opt} = \frac{2}{1 + \sqrt{1 - \rho^2}}$$

Also in tables 1 and 2 are the optimal relaxation factors calculated from this formula along with those found experimentally. For the 1-D problem the prediction of omega is very good and fortunately is best when the overlap is smallest, i.e. when there is the most to gain and the choice of relaxation factors is most critical. In the 2-D problem the prediction of omega is not as good as in the 1-D problem, but the sensitivity of the savings to the choice

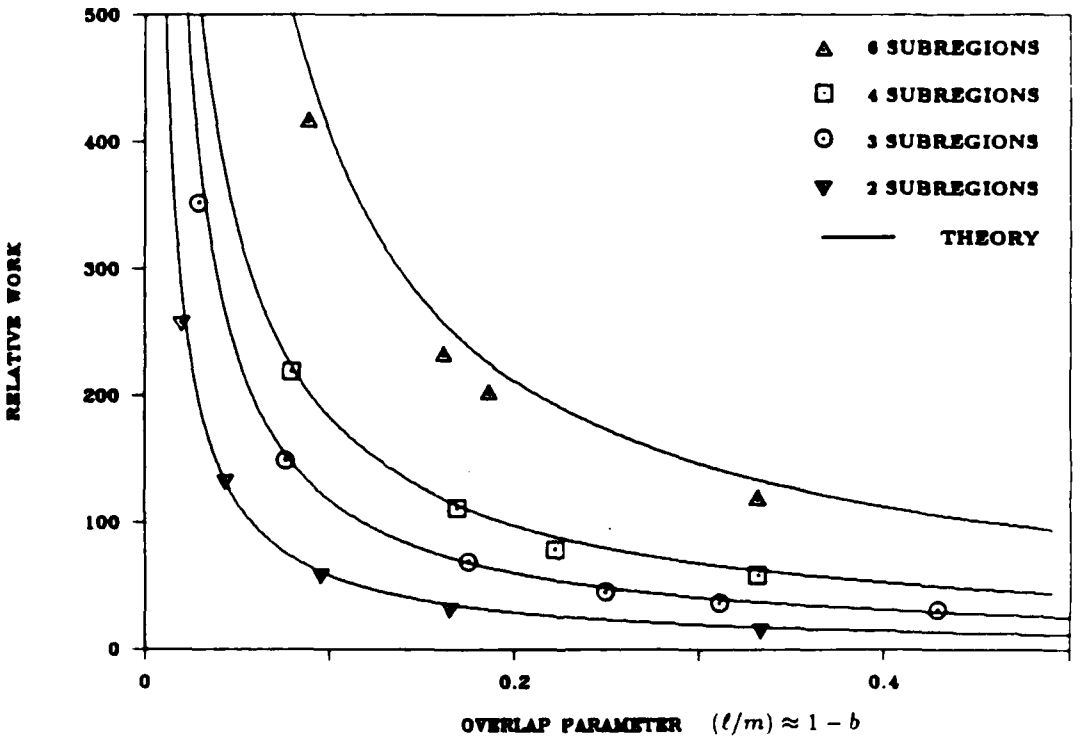

Figure 5: Theoretical and computational estimates of the relative work for the 1–D case using no relaxation. The work is relative to that needed to solve once on a single grid over the entire domain. Solution work is proportional to the number of points on a grid.

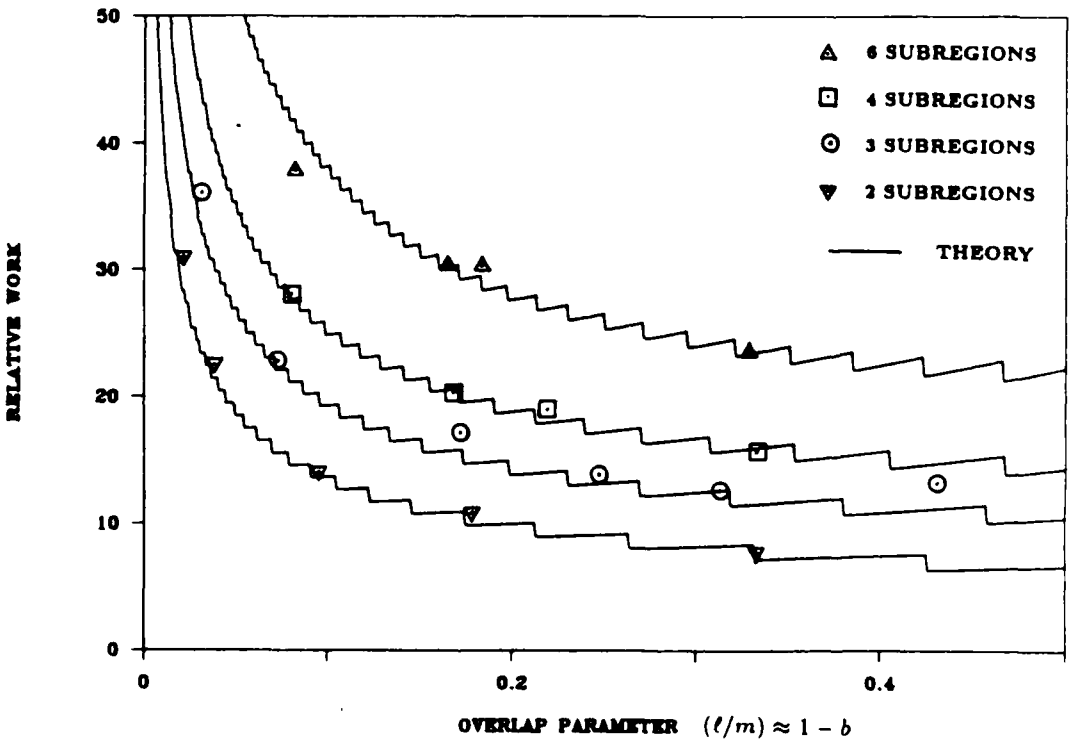

Figure 6: Theoretical and computational estimates of the relative work for the 1–D case using optimal overrelaxation.

of omega is much less in the 2-D problem, and again, as in the 1-D case, the prediction of the optimal relaxation factor is better as the sensitivity increases. Almost all of the computational savings can be realized using the theoretically predicted optimal relaxation factors in both the 1 and 2-D problems!

Other methods of increasing the convergence rate of the $\mathcal{SAM}$ problem can involve changing the order of the solution of the subregions for cases where there are more than two subregions. Two possibilities are investigated. The first involves sweeping forward (as in $\mathcal{SAM}$) and then sweeping backwards along the row of overlapping grids, and hence can be thought of as an SSOR (symmetric SOR) technique. The second procedure uses a Black-Red solution pattern, solving on every other grid during the first step and then solving on the remaining grids the second step.

Sweeping in both directions (SSOR) produced little to no gain in efficiency compared with the standard $\mathcal{SAM}$, and in some cases requires more computational effort to produce a converged solution. When combined with overrelaxation it does not produce as dramatic savings as does the $\mathcal{SAM}$ with overrelaxation, but the choice of relaxation factor is less critical. There is no great advantage which leads one to choose SSOR over SOR.

The Black-Red solution technique produced results almost identical to the $\mathcal{SAM}$ results for both the unrelaxed and overrelaxed methods. The computational savings and optimal relaxation factor are the same for a given problem and hence the theoretical determination of the overrelaxation factor can be used with the B-R scheme. The major difference between the $\mathcal{SAM}$ and the B-R method is that in the $\mathcal{SAM}$ one can solve on only one subregion at any time, for its solution is necessary to set boundary conditions for the next subregion. Using the B-R scheme one can solve on up to half the subregions at any one time, each one being completely independent of the others for it is only the next set of grids that needs these solutions for setting boundary conditions. Thus the B-R scheme is ideal for multi-processor machines.

Acknowledgement: The authors acknowledge Steve Caruso's participation in the early stages of this project and his helpful discussions.

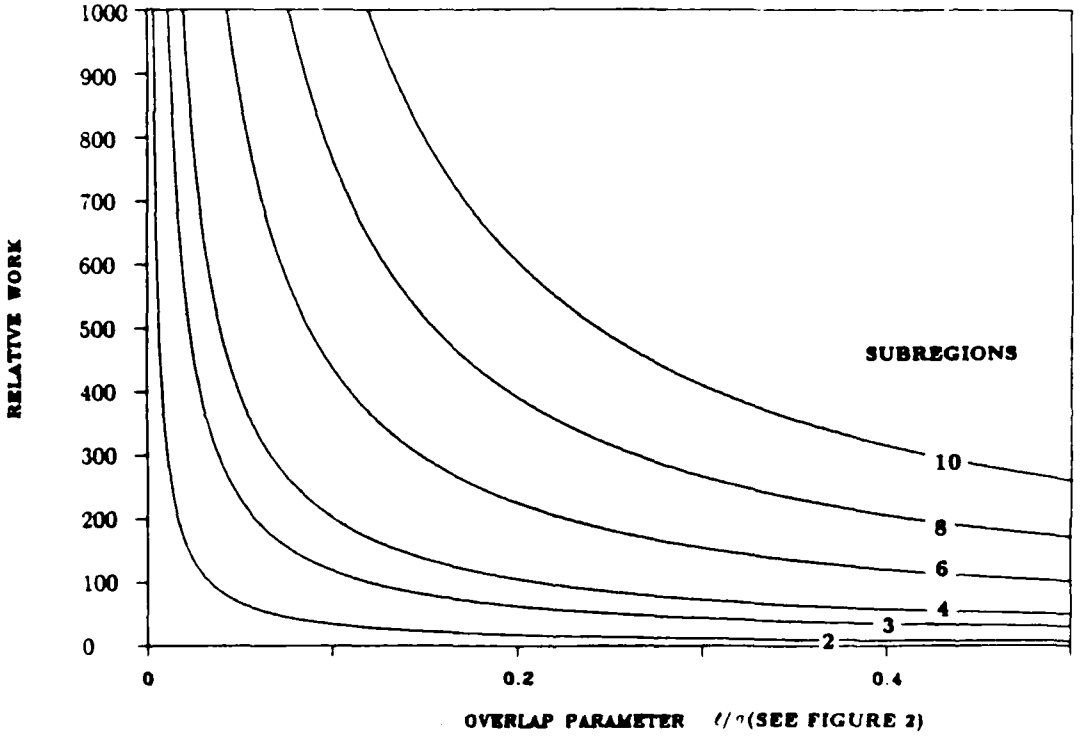

Figure 7: Theoretical estimates of the relative work for 2-D case using no relaxation and holding the domain size constant.

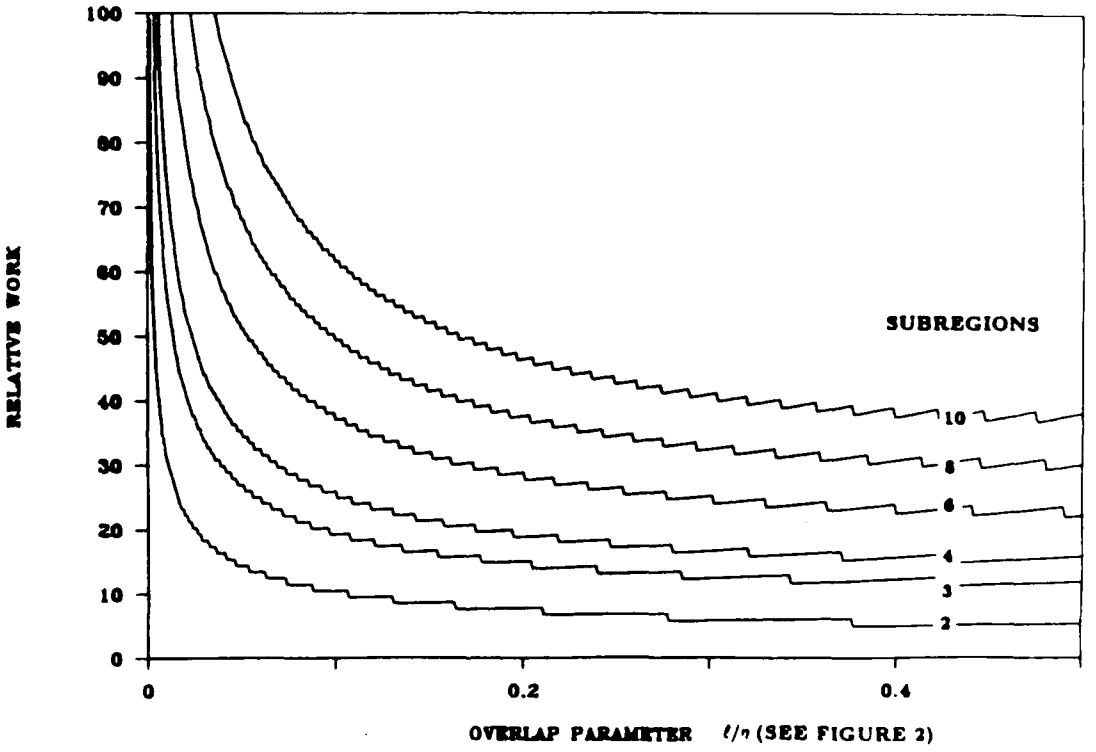

Figure 8: Theoretical estimates of the relative work for the 2–D case using optimal overrelaxation and holding the domain size constant.

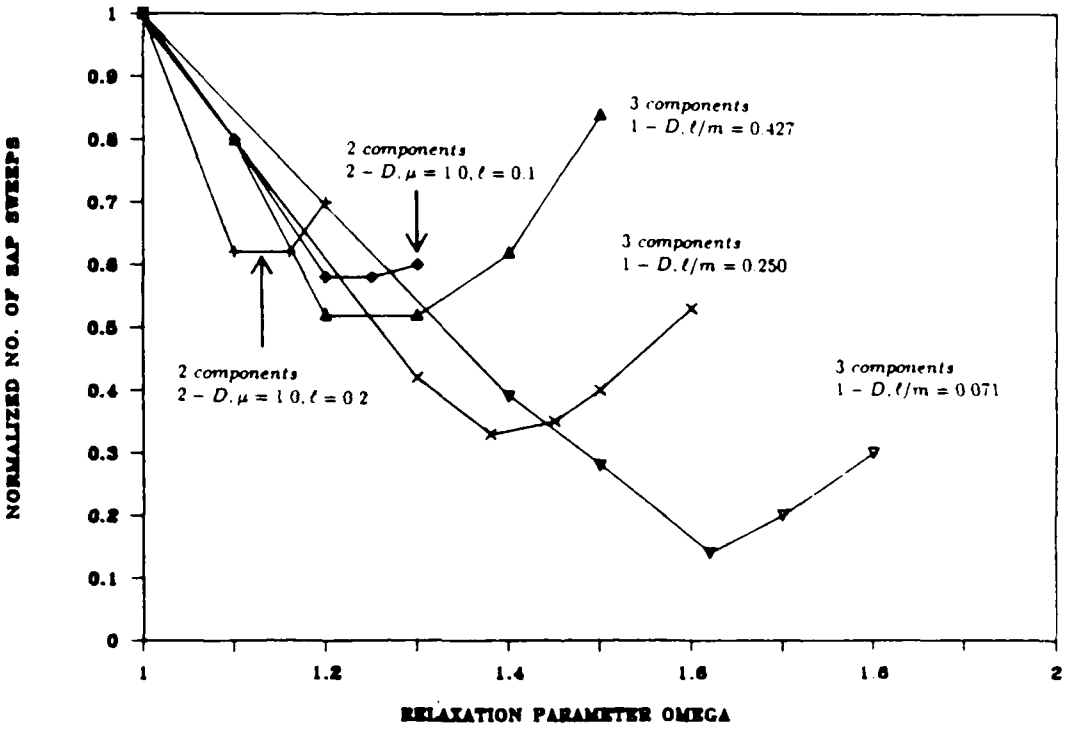

Figure 9: Relative work (work normalized by work needed using no relaxation) for various 1–D and 2–D problems as a function of the overrelaxation parameter omega.

1-D Model Problem Results					
number of subregions	l/m	S_A^M	S_A^M + SOR	optimal ω observed	optimal ω from theory
2	0.333	14	7	1.2	1.15
	0.182	27	10	1.3	1.27
	0.095	52	14	1.42	1.40
	0.039	129	22	1.60	1.57
	0.019	258	30	1.68	1.67
3	0.427	19	10	1.3	1.21
	0.309	26	10	1.3	1.28
	0.250	37	12	1.38	1.33
	0.175	66	16	1.48	1.44
	0.071	141	21	1.62	1.58
	0.030	349	35	1.71	1.71
4	0.333	44	12	1.42	1.36
	0.220	70	16	1.5	1.46
	0.167	97	18	1.52	1.51
	0.083	204	26	1.67	1.63
5	0.333	88	17	1.55	1.50
	0.190	169	26	1.62	1.61
	0.167	193	26	1.65	1.64
	0.083	397	36	1.75	1.74

2-D Model Problem Results					
number of subregions	$\mu = 1$ κ	S_4M	S_4M + SOR	optimal ω observed	optimal ω from theory
2	0.4	5	4	1.05	1.02
	0.3	6	5	1.08	1.04
	0.2	8	5	1.12	1.08
	0.1	15	7	1.2	1.19
	0.05	30	12	1.35	1.32
3	0.4	6	5	1.05	1.05
	0.3	7	6	1.05	1.06
	0.2	10	6	1.1	1.11
	0.1	18	9	1.22	1.21
	0.05	35			
4	0.4	7	5	1.05	1.05
	0.3	8	6	1.1	1.06
	0.2	11	7	1.15	1.11
	0.1	20	9	1.25	1.21
	0.05	35			
5	0.4	8	6	1.05	1.05
	0.3	7	6	1.05	1.06
	0.2	10	6	1.1	1.11
	0.1	18	9	1.22	1.21

*Bibliography

[CFO85] S. Caruso, J. Ferziger, and J. Oliger. *Adaptive Grid Techniques for Elliptic Fluid-Flow Problems.* Technical Report, Stanford University, Center for Large Scale Scientific Computation, 1985.

[Mil65] K. Miller. Numerical analogs to the schwarz alternating procedure. *Numerische Mathematik* 7:91–103, 1965.

[Sch69] H. A. Schwarz. Ueber einige abbildungsaufgaben. *Jour. f. die reine und angew. Math.* 70:105–120, 1869.

[Sta77] G. Starius. Composite mesh difference methods for elliptic boundary value problems. *Mumerische Mathematik*, 28:243–258, 1977.

[Tan86] Wei-Pai Tang. *Schwarz Splitting and Parallel Computations.* PhD thesis, Stanford University, Computer Science Dept. Stanford, CA 94305, 1986.

[Vol68] E. Volkov. *The Method of Composite Meshes for Finite and infinite Region with Piecewise Smoth Boundary.* Technical Report 96. Steklov Institute of Mathematics, 1968.

[You71] D. M. Young. *Iterative solution of large linear system.* Academic Press, 1971.

END

12-86

DTIC